Vidakis *et al. Biochar* (2025) 7:22
https://doi.org/10.1007/s42773-024-00400-8

Biochar

ORIGINAL RESEARCH Open Access

Enhancing biocomposite critical quality indicators (CQIs): the impact of biochar content in additive manufacturing

Nectarios Vidakis[1], Markos Petousis[1*], Dimitrios Sagris[2], Constantine David[2], Nikolaos Mountakis[1], Mariza Spiridaki[1], Emmanuel Maravelakis[3], Costas Charitidis[4] and Emmanuel Stratakis[5,6]

Abstract

Biocomposite filaments for material extrusion (MEX) additive manufacturing, particularly those derived from agricultural biomass, have attracted significant research and industrial interest. Biochar is a well-documented reinforcement agent that is used in several polymeric matrices. However, systematic research efforts regarding the quality scores of parts built with MEX 3D printing with biochar-based filaments are marginal. Herein, the impact of biochar loading on the quality metrics of the five most popular polymers for MEX 3D printing (ABS, HDPE, PETG, PP, and PLA) is quantitatively examined in depth. Sophisticated and massive Non-Destructive Tests (NDTs) were conducted, and the impact of biochar loading on the critical quality indicators (CQIs), including porosity, dimensional conformity, and surface roughness, was documented. The quality scores for the biochar filler loading, also five in total, were statistically correlated with the corresponding reinforcement metrics for the five polymeric matrices. A statistically significant antagonistic interaction between the tensile strength course and porosity/dimensional deviation metrics, particularly for PETG, was observed. It can be concluded that the lowest porosity and dimensional deviation are associated with the highest strength. The 4 wt% biocomposite exhibited optimal quality performance in most polymers studied.

Highlights

- Comparison of the effects of biochar on five polymeric matrices in additive manufacturing: Acrylonitrile Butadiene Styrene (ABS), High Density Polyethylene (HDPE), Polyethylene Terephthalate Glycol (PETG), Polypropylene (PP), and Polylactic Acid (PLA).
- Quality metrics (surface roughness, porosity, and dimensional accuracy) were compared and correlated with mechanical response.
- Low porosities and dimensional deviations were detected in the 4 wt% polymer/biochar composites, having the highest tensile strength among the composites tested.

Keywords 3D printing, Biochar, Polymers, Material extrusion (MEX), Micro-computed tomography (μ-CT), Atomic force microscopy (AFM)

*Correspondence:
Markos Petousis
markospetousis@hmu.gr
Full list of author information is available at the end of the article

Graphical abstract

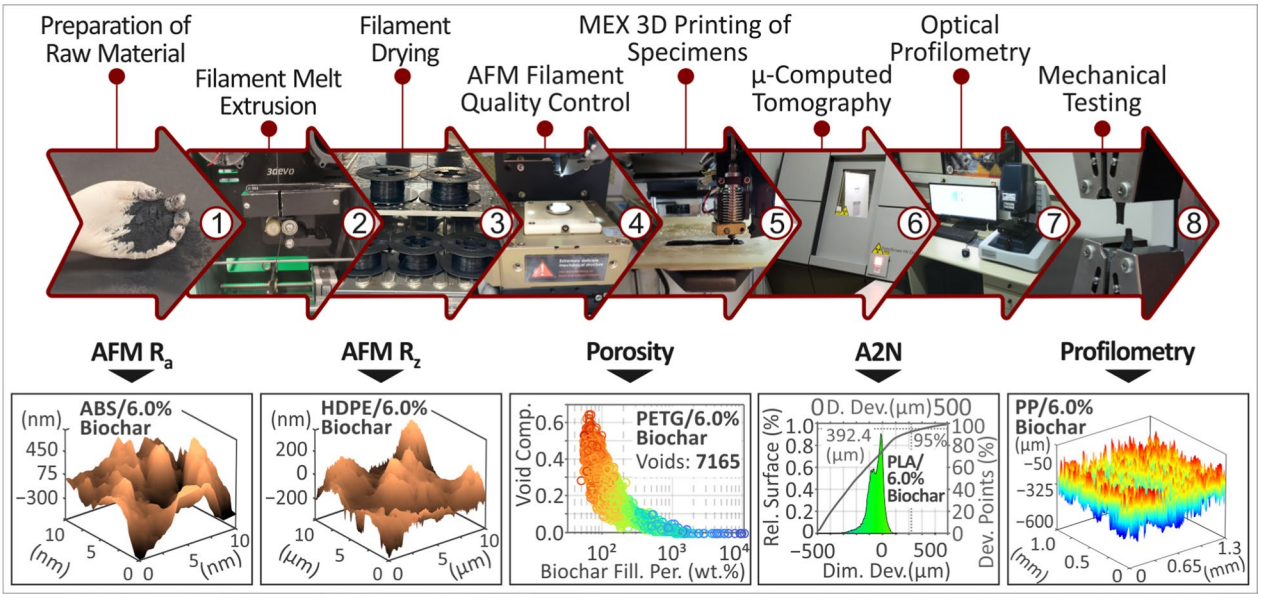

1 Introduction

Additive manufacturing (AM) technology is used to build structures of various shapes by placing one layer of material on top of the other (Ngo et al. 2018). Every potential application of AM requires distinct properties that can be obtained by selecting appropriate material and printing parameters (Mayakrishnan et al. 2023). AM is one of the most promising and rapidly growing technologies for fabricating polymeric composite structures (Nikzad et al. 2011; Serra et al. 2013; Tekinalp et al. 2014; Wei et al. 2015; Postiglione et al. 2015; Kalsoom et al. 2016; Mohamed et al. 2016; Tian et al. 2016; Miller et al. 2017; Idrees et al. 2018). Different matrix materials, such as polypropylene (PP) (Michailidis et al. 2024), acrylonitrile butadiene styrene (ABS) (Vidakis et al. 2023c), polyamide 12 (Nasikas et al. 2024), polylactic acid (Vidakis et al. 2024a), polyethylene terephthalate glycol (PETG) (Petousis et al. 2024b), and high-density polyethylene (HDPE) (Petousis et al. 2024c) have been investigated for their efficacy in the AM technology. A wide variety of additives such as copper (Vidakis et al. 2024b), carbon (Vidakis et al. 2023d), and ceramics (Vidakis et al. 2023e) have also been examined. The quality of 3D-printed items was studied with the aim of improving it by finding the optimum 3D printing settings (Vidakis et al. 2023a; 2024C).

The use of biochar-based polymer composites offers the opportunity to utilize environmentally-friendly and sustainable materials (Ahmetli et al. 2013; Snowdon et al. 2014; Das et al. 2015; Anerao et al. 2023), potentially replacing conventional non-biodegradable polymer composites (George et al. 2023). According to the literature, environmentally-friendly materials are designed to minimize the environmental impact of human activities (Elfaleh et al. 2023). These materials are typically sustainable, renewable, and biodegradable and reduce energy consumption, waste, and pollution. Biochar (Falliano et al. 2020) is a carbon-rich by-product known for its non-toxicity, sustainability, renewability, positive environmental impact, and unique inherent properties (Shanmugam et al. 2022; Mayakrishnan et al. 2023). Owing to its porous nature and highly functionalized surface, this material provides nucleation sites for chemical reactions and is compatible with cement, asphalt, and other polymers (Zhang et al. 2022). The Biochar Market Size is valued at USD 515.9 Mn in 2022 and is predicted to reach USD 1,385.2 Mn by the year 2031 at an 11.7% CAGR during the forecast period for 2023–2031 (Insight ace analytic 2024).

There are three different methods of biochar production: pyrolysis, gasification, and hydrothermal carbonization. Biochar can possess different physical and chemical properties depending on the fabrication conditions, such as the heating rate, pyrolysis temperature, time of residence, gas pressure, pyrolytic atmosphere, and types of biomass waste (Leng and Huang 2018; Maljaee et al. 2021; He et al. 2022). It can be produced by the pyrolysis of different waste materials, such as food, wood, manure, and agricultural waste, as well as municipal and

industrial sludge (Zhang et al. 2022), at temperatures between 400 °C and 700 °C in an oxygen-free atmosphere (Li et al. 2020). Waste materials are carbonized at high temperatures and combined as fillers to provide a high surface area and hardness, as well as competent behavior for thermal loading (Das et al. 2021).

Biochar has gained attention because of its environmental benefits and potential as a component of building materials, soil improvement, and water filtration. The physical performance of biochar-based materials varies depending on the biomass source, pyrolysis conditions, and intended applications (Cosentino et al. 2019). In resins, an increase of up to 63% in the ultimate tensile strength had been reported (Giorcelli et al. 2019). The thermal properties of epoxy resins were also improved by biochar addition (Minugu et al. 2021). Biochar is also used in concrete composites, achieving an almost 20% improvement n flexural strength (Akhtar and Sarmah 2018). These findings demonstrate that biochar can be a valuable eco-friendly filler for various materials. Applications of biochar include agriculture, particularly to enhance soil structure, improve fertility in degraded soils, and increase soil water retention (Hagemann et al. 2017). Additionally, other emerging applications such as additives and raw materials in construction can be developed by adjusting the surface functionality, porous structure, and aromatic/graphitic carbon composition with designs for specific usage (Sajjadi et al. 2019; Maljaee et al. 2021; Chen et al. 2022).

Growing environmental awareness is driving the search for alternatives to nonrenewable materials. Consequently, numerous biodegradable materials are being continually developed (Ho et al. 2015). In this study, and for the first time, to the best of our knowledge, we compared the impact of biochar on five different polymers, acrylonitrile butadiene styrene (ABS) (Lee et al. 2005; Ziemian et al. 2015), polyethylene terephthalate glycol, high-density polyethylene (HDPE), polylactic acid (Afrose et al. 2016; Chacón et al. 2017; Laureto and Pearce 2018) and Polypropylene (PP) (Joseph et al. 2002; Wambua et al. 2003; Pervaiz and Sain 2003; Sain et al. 2005; Shubhra et al. 2011; Carneiro et al. 2015) on the quality of 3D-printed parts and correlated the findings with the mechanical performance of the parts. These five polymers were selected for this study because they possess a high market share among the polymers used for 3D printing (Almuallim et al. 2022).

ABS has been widely used in 3D printing for several years because of its low cost and excellent mechanical properties, (Dhakal et al. 2023) such as toughness, impact resistance, and elevated glass transition temperature (Torrado Perez et al. 2014). HDPE is a thermoplastic that is exceptionally resistant to heat and cold and is chemically stable, mechanically strong, and electrically insulating (Musa et al. 2017). Moreover, it exhibited dimensional stability and flame resistance (Zhang et al. 2020). Some of its characteristics are low density (in the range of 950 and 970 kg m^{-3}), high tensile strength of high levels (in the range of 20 and 32 MPa), flexibility (Lukkassen and Meidell 2003; Andersen et al. 2015; Geyer et al. 2017), melting point, and ignition temperature of 130 °C and 487 °C, respectively (Alauddin et al. 1995). HDPE can be applied in diverse fields such as manufacturing, agriculture, and automotive industries (Dusunceli and Colak 2008). They can be found in the form of films, wire insulation, wires, containers, sheets, and pipelines (Yasmin and Daniel 2004). In addition, it is recyclable and affordable (Achilias et al. 2007; Autoeuropa 2017). Polyethylene terephthalate glycol (PETG) is a copolyester-based polymer (Guessasma et al. 2019) derived from polyethylene terephthalate (PET). Unlike PET, the added glycol did not exhibit strain-induced crystallization(Dupaix and Boyce 2005). They are highly transparent (Guessasma et al. 2019; Yuan et al. 2019), and have high toughness (Petrov et al. 2021), adequate mechanical and chemical properties (Li et al. 2009; Badia et al. 2012), heat resistance, and high ductility (Bichu et al. 2023). It is considered a biomaterial owing to its cost-effectiveness and biocompatibility (Yan et al. 2024). PETG has applications in industries related to medicine (Yan et al. 2024), food, clamshells, blister packs, cosmetic packing, hot-fill containers, and display cases (Paszkiewicz et al. 2017; Habel et al. 2018; Durgashyam et al. 2019; Bałdowska-Witos et al. 2020), and engineering (Szykiedans et al. 2017). Polylactic acid (PLA) is a linear aliphatic polyester (Ho et al. 2015).

It is a biodegradable material (Taib et al. 2023) that can be produced using renewable sources. Biodegradable thermoplastics are the ones that reduce the environmental impact of petroleum-based polymers, which also contributes to the eco-friendliness of a material and PLA complies with this definition. Based on the definition of environmentally-friendly materials provided above, PLA is often mentioned in the literature as an eco-friendly material because of its nature (Hussain et al. 2015), as it is usually sourced from nature-based resources. Its range of applications varies among biomedicals, textile fibers, packaging, and technical items (Couture et al. 2016; Murariu and Dubois 2016). In addition to its characteristic of being biodegradability, it is eco-friendly, recyclable (Drumright et al. 2000; Sawyer 2003), biocompatible (Gupta et al. 2007; Rasal et al. 2010), processable (Auras et al. 2004), and energy-efficient (Rasal et al. 2010). Polypropylene (PP) is a thermoplastic polymeric material that results from propylene molecule polymerization. The crystallinity level of PP was between the amplitudes of 40% and 60% (Joseph et al. 2002), and the melting point

ranged between 60°C and 166 °C (Somani et al. 2002). Some of its properties include transparency, high heat-distortion temperature, dimensional stability, and flame resistance (Shubhra et al. 2013).

The abovementioned polymers were combined individually with biochar particles as additives in five composites of 2.0–10.0 wt% filler percentages each (a 2 wt% step was set for the content increase between the compounds). The exact filler content was used in each polymer and composites were prepared with the exact same process to have as reliable as possible comparable results. The composite mixtures were extruded into filaments, and filaments of pure polymeric materials were produced as control samples. Subsequently, specimens from each filament type were 3D-printed, providing a total of three hundred (300) samples tested during the entire study. The fabricated samples were subjected to a series of measurements related to porosity, A2N dimensional deviation, and surface roughness. The porosity is due to the 3D printing structure of the samples. Even with 100% infill density, the 3D printing structure by its nature has internal pores. This is a well-known and studied issue in 3D-printed parts and can vary depending on various parameters, such as the material and 3D printing settings. This porosity has an impact on the mechanical properties of 3D-printed parts (Wang et al. 2019). In this study, the effect of the biochar content of the composites on the porosity of 3D-printed parts was investigated and presented. These findings correlate with the mechanical properties of the samples. Optical profilometry was used to obtain R_a and R_z metrics (surface roughness). Five measurements were obtained for each specimen sample, which also occurred for the atomic force microscopy (AFM) R_a and R_z metrics for each filament sample. One thousand and fifty (1050) tests were conducted on specimens, and one seven hundred fifty (750) tests on filaments, making a total of one thousand eight hundred (1800) tests conducted during the entire study. The aforementioned work constituted approximately 750 GB of the test results. The measured values were significantly higher. For example, two values were obtained for each AFM measurement (Ra and Rz). Following these tests, the quality of the 3D-printed examples was evaluated and correlated with their tensile strength to find possible connections. The findings are expected to have high merit in industrial applications, as they can lead to 3D-printed parts with improved quality for composites with these five polymers as matrix materials (ABS, HDPE, PETG, PP, PLA) and biochar as the additive. Biochar complies with the definition of environmentally-friendly materials as it comes from nature-based waste (Vidakis et al. 2023b). Therefore, an eco-friendly additive has been studied for the development of polymeric composites. The effect of biochar on different matrices was evaluated and compared for the first time, as mentioned above, and the correlation with the mechanical performance was explored.

2 Materials and methods

Figure 1 describes the processes performed in this study in an image form. Initially, all the raw materials were placed in an industrial oven to dehydrate overnight (Fig. 1a). The melt extrusion of the filaments followed after material mixing in predefined quantities (Fig. 1b). The filaments were left overnight for dehydration (Fig. 1c). The filaments were used to supply the 3D printing procedure of material extrusion (MEX) for the examples (Fig. 1d), which were later quality-controlled and inspected (Fig. 1e). The produced specimens underwent micro-CT scanning (Fig. 1f) as part of their examination and were investigated using optical profilometry (Fig. 1g). Mechanical tests were then conducted on the samples and the outcomes were evaluated (Fig. 1h).

2.1 Materials

This study used five different polymeric materials: ABS, HDPE, PETG, PLA, and PP. Biochar was used as the filler. The suppliers from which the polymeric materials were purchased are as follows:

- Acrylonitrile butadiene styrene (ABS) polymeric powder was obtained from INEOS Styrolution (Frankfurt, Germany) grade Terluran Hi-10 with a density of 1080 kg m^{-3} and a tensile strength of 38 MPa.
- Industrial grade High-Density Polyethylene (HDPE) Kritilen powder, from Plastika Kritis S.A., Heraklion, Greece, possessing 7.5 g 10 min^{-1} mass-flow rate, 0.960 g cm^{-3} density, and 127 °C Vicat softening temperature.
- Polyethylene Terephthalate Glycol (PETG) was purchased from Felfil Srl (Torino, Italy).
- Polylactic Acid (PLA) 3052D grade, from Plastika Kritis SA, located in Heraklion, Greece, possesses 116,000 g mol^{-1} molecular weight, 62 MPa (ASTM D638) tensile strength at yield, 153 °C (ASTM D 3418) melting temperature, 57.5 °C (ASTM E1356) glass transition temperature, and 4 g/10 min (ASTM D1238) melt flow index.
- Polypropylene (PP) in powder was obtained from Hellenic Petroleum S.A., located in Athens, Greece (Ecolen PP trademark), and had a melt volume flow rate of 34 cm^3/10 min (ISO 1133:2005).

Regarding the biochar material, olive tree pruning was performed, and impurities were removed by washing and air-drying the prunings. Biochar was produced

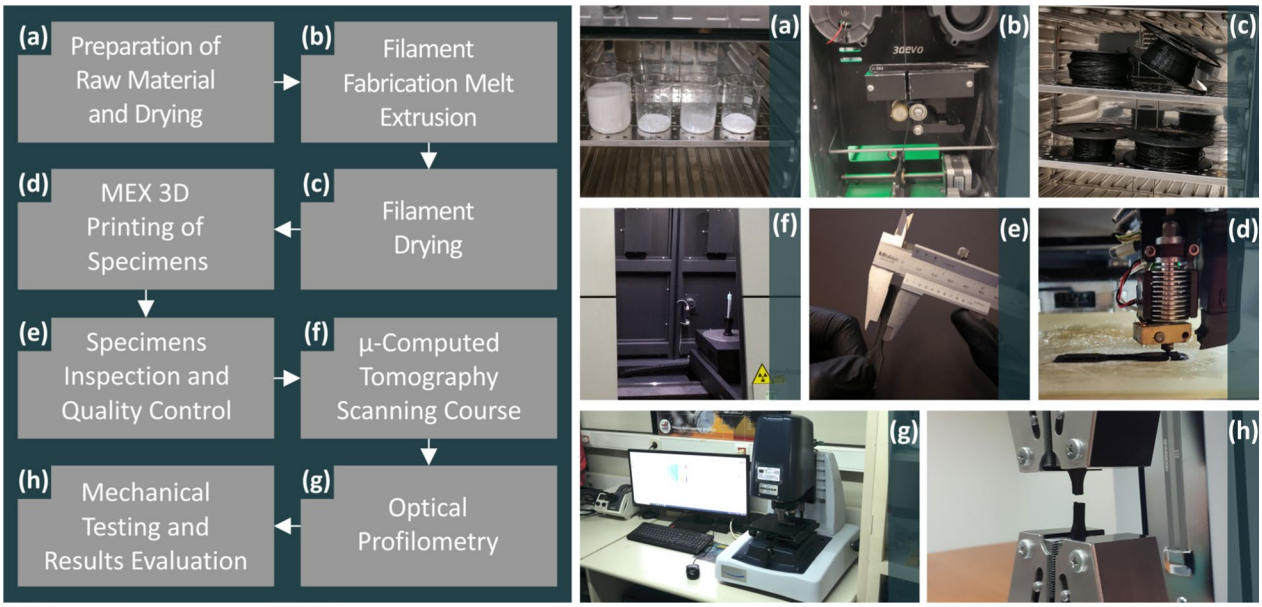

Fig. 1 Summary of the procedures employed in the work herein: **a** the dehydration of raw materials, **b** melt extrusion of the filaments and **c** their dehydration, (4) MEX 3D specimens' fabrication, as well as **e** their inspection and quality control, **f** micro-CT scanning **g** optical profilometry investigation, and **h** examination of the samples' mechanical behavior

by flame-curtain pyrolysis. Details of the pyrolysis kiln materials, design features, and dimensions required for this study can be found in the available literature (Tsubota et al. 2021).

The process was initiated by dividing the prunings into three different batches and then conducting flame-curtain pyrolysis in triplicate for approximately 1 h (each) at 540 ± 50 °C. According to the literature, the temperature variation can be large in this type of reactor (Jayakumar et al. 2023). Therefore, four thermocouples attached at four different locations on the external surface of the kiln were used to monitor the temperature. It should be noted that some temperature fluctuations occurred during the initial flame cap establishment period. Nevertheless, both the pruning feeding rate (layering process) and temperature (to a large extent) were stabilized.

Feedstock uniformity and optimum feeding rate are vital for the reduction of temperature fluctuations, for the most part, in flame cap pyrolysis. By the time the pyrolysis of the first pruning started, a heating source (external) was not necessary, and the procedure was self-sustained. Water quenching of each biochar batch was followed by a 96 h air-drying and weighing. One sample was prepared from the three samples and homogenized. The same example is ground using a sepor-type rod mill. Further details can be found in the literature (Tsubota et al. 2021) and supplementary files of the study. The efficiency of pyrolysis of olive tree pruning was found to be 22% (Vidakis et al. 2023b), which is in agrement with the literature on the pyrolysis of woody waste (Jayakumar et al. 2023). The characteristics of the specific biochar used were presented in detail in a previous study by the research team (Tsubota et al. 2021). The physical and chemical properties of the specific biochar from olive trees were also presented in a previous study by this research group (Nikolopoulos et al. 2023). Further details about the olive tree biochar preparation process have already been presented in the two aforementioned works and in one more work of our research group (Vidakis et al. 2023b).

2.2 Biochar inspection

The biochar material was inspected by scanning electron microscopy (SEM), and the acquired images were illustrated in Fig. 2d and e, at 1000× and 10,000× magnification, respectively. For the SEM analysis, a JEOL JSM 6362LV (JEOL Ltd., Peabody, MA, USA) electron microscope was used.

2.3 Material extrusion filaments

The filament fabrication was performed using a mixture of multiple biochar-filler percentages. The extrusion was carried out using an extruder model named 3devo Composer (single-screw, by the 3devo B.V. company, located in Utrecht, The Netherlands), which produced a filament of 1.75 mm diameter, which is considered suitable for the 3D printing process of MEX. The fabricated filaments were quality-controlled, inspected using AFM, and mechanically tested.

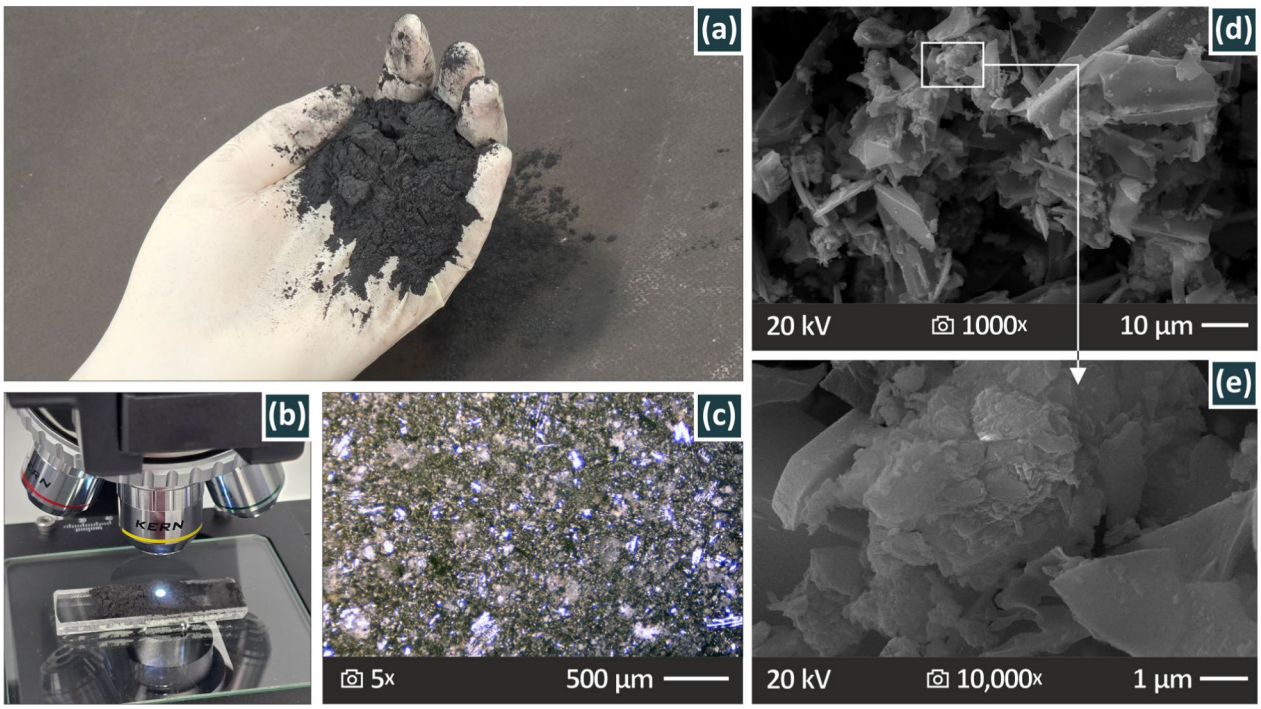

Fig. 2 Examination of biochar particles: **a** picture of the raw material, **b** optical microscopy examination of the biochar powder and **c** the respective captured picture, **d, e** SEM images magnified respectively at 1000× and 10,000×

2.4 Surface roughness

AFM and optical profilometry were employed to determine the Ra and Rz values of the topographies of the compounds. The methodology for the AFM measurements (PPP-NCHR tip from Nanosensors, Neuchatel, Switzerland) (Vidakis et al. 2023b) and optical profilometry (Bruker Contour GT-K 3D Optical Microscope, Bruker Nano Surfaces Division, Tucson, AZ, USA) was derived from the literature (Vidakis et al. 2024c). Five measurements were taken for each sample, and the mean Ra and Rz were calculated. Overall, a laborious effort with 750 surfaces measured was performed for the two surface roughness metrics (five measurements in five examples per case, six recipes, and five materials: 5×5×6×5=750, 1500 values in total for Ra and Rz). Please refer to the supplementary file for the study.

2.5 MEX 3D-Printing

After filament production and inspection, they were used for the MEX 3D-printing procedure. The apparatus used for this purpose was an Intamsys Funmat HT (Intamsys, Shanghai, China). As shown in Fig. 3a, the chosen printing settings were ±45° printing orientation (90 deg shift between successive layers to reduce anisotropy), 0.2 mm layer thickness, 2 perimeters (on the outside), 100% fill density, and 40 mm s^{-1} travel speed. The manufactured specimens were dog-bone-shaped. Samples from the tensile-fabricated specimens are shown in Fig. 3c, along with an image captured during the tensile testing. Moreover, the σ_b mean values for ABS, HDPE, PP, PETG, and PLA for all biochar filler percentages (0.0, 2.0, 4.0, 6.0, 8.0, and 10.0 wt%) are shown in Fig. 3b. The creation of the curves presented in Fig. 3b was based on five measurements taken from each polymer's six formulas, which were then considered to produce their average value and result in the curves.

It should be mentioned that the results related to ABS (Vidakis et al. 2024d), HDPE (Vidakis et al. 2024e), PLA (Vidakis et al. 2023b), and PP (Petousis et al. 2024a) were derived from corresponding studies that have already been conducted and can be found in the literature. The PLA/biochar study was expanded to include PLA/biochar 10.0 wt% composite, which was not included in the already published investigation. This information was acquired by further examination of the specific filler percentage following the same procedures, standards, and settings. PETG/biochar polymer data were obtained using the same series of procedures, tests, and examinations for five different filler quantities (2.0, 4.0, 6.0, 8.0, and 10.0 wt%).

2.6 Optical microscopy examination

The specimens were inspected for their structural and morphological characteristics using optical microscopy, which

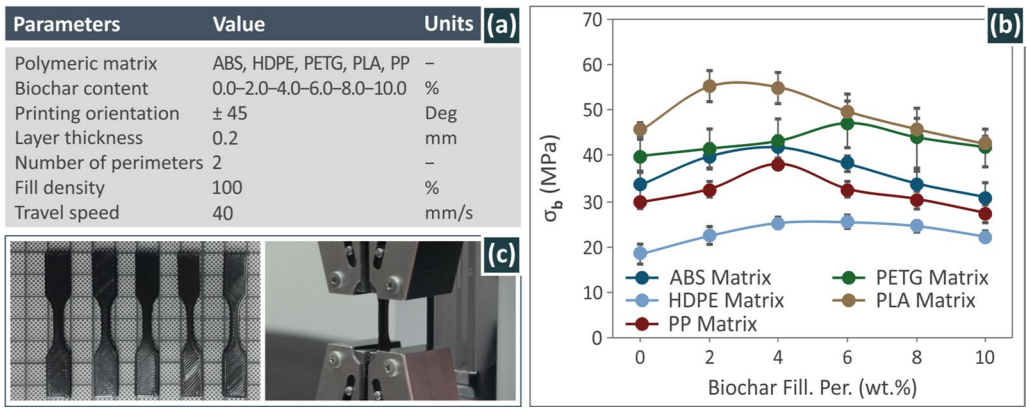

Fig. 3 **a** Presentation of the 3D tensile specimens' printing parameters, accompanied by the respective values and units, **b** σ_b mean values, derived from the respective studies existing in the literature, regarding the ABS (Vidakis et al. 2024d), HDPE (Vidakis et al. 2024e), and PP (Petousis et al. 2024a), as well as PLA (Vidakis et al. 2023b) (which was expanded) and PETG (which has been studied but not published yet) for all biochar filler percentages (0.0, 2.0, 4.0, 6.0, 8.0 and 10.0 wt%), **c** some randomly chosen fabricated tensile specimens and an image captured during the tensile testing procedure

was conducted using a microscope OKO 178 (by the company KERN & SOHN GmbH, Balingen, Germany). The pictures were captured with a digital camera featuring a 5MP resolution, model ODC 832 (KERN & SOHN GmbH, Balingen, Germany). Images of the 3D-printed examples were created by capturing multiple images, which were later compared with the derived μ-CT results.

2.7 Micro-computed tomography

The structures of the specimens were also investigated using micro-CT, and the results were evaluated. More specifically, the porosity and geometrical accuracy of the 3D-printed examples were examined by scanning the respective 3D printing structure. The methodology was taken from the literature (Vidakis et al. 2023a; 2024c). Please refer to the supplementary file for the study.

2.8 Correlation of the results

The Pearson correlation coefficient (Pearson and Galton 1997) was applied to determine the correlation between the quality metrics and the reinforcement capabilities of the five polymers (presented in other studies, ABS (Vidakis et al. 2024d), HDPE (Vidakis et al. 2024e), PP (Petousis et al. 2024a), PLA, (Vidakis et al. 2023b) which was expanded, and PETG, which has been studied but not published yet). The equation is given by the formula (Lee Rodgers and Nicewander 1988)

$$r = \frac{\sum (x_i - \bar{x})(y_i - \bar{y})}{\sqrt{\sum (x_i - \bar{x})^2 \sum (y_i - \bar{y})^2}} \quad (1)$$

where r is the correlation coefficient (linear relation between x and y); x_i is the x variable value; y_i is the respective y variable value; $\bar{x}$ and $\bar{y}$ are the mean values of the variables. The r coefficient values were in the range of $-1 < r < 1$ (Asuero et al. 2006; Sedgwick 2012):

- Positive values show a positive relationship between the variables, that is, the increase in one parameter increases the other as well.
- The zero r-value shows no correlation between the variables.
- Negative r values indicate a negative correlation, that is, an increase in one parameter decreases the other.

3 Results

3.1 AFM characterization of the filaments

Figure 4 summarizes the results obtained from the AFM characterization of the filaments. Figure 4a shows the surface topology of the filaments made with all five compounds (of the five polymers) with 6 wt% biochar percentage. Figure 4b and c illustrate the mean values of the R_z and R_a metrics, respectively, measured for ABS, HDPE, PETG, PP, and PLA/biochar (0.0–10.0 wt%) composite filaments. In the PETG, ABS, and PP/biochar compounds, the lowest R_a and R_z roughness values were observed for the one with 10.0 wt% filler quantity, while the lowest R_a and R_z values for the HDPE and PLA/biochar composites were found in the neat polymers. In the ABS polymer, the addition of biochar had a low impact on surface quality, as determined by AFM. The increase in the surface roughness was more intense for the other polymers. For PP and PETG, the lowest value was found

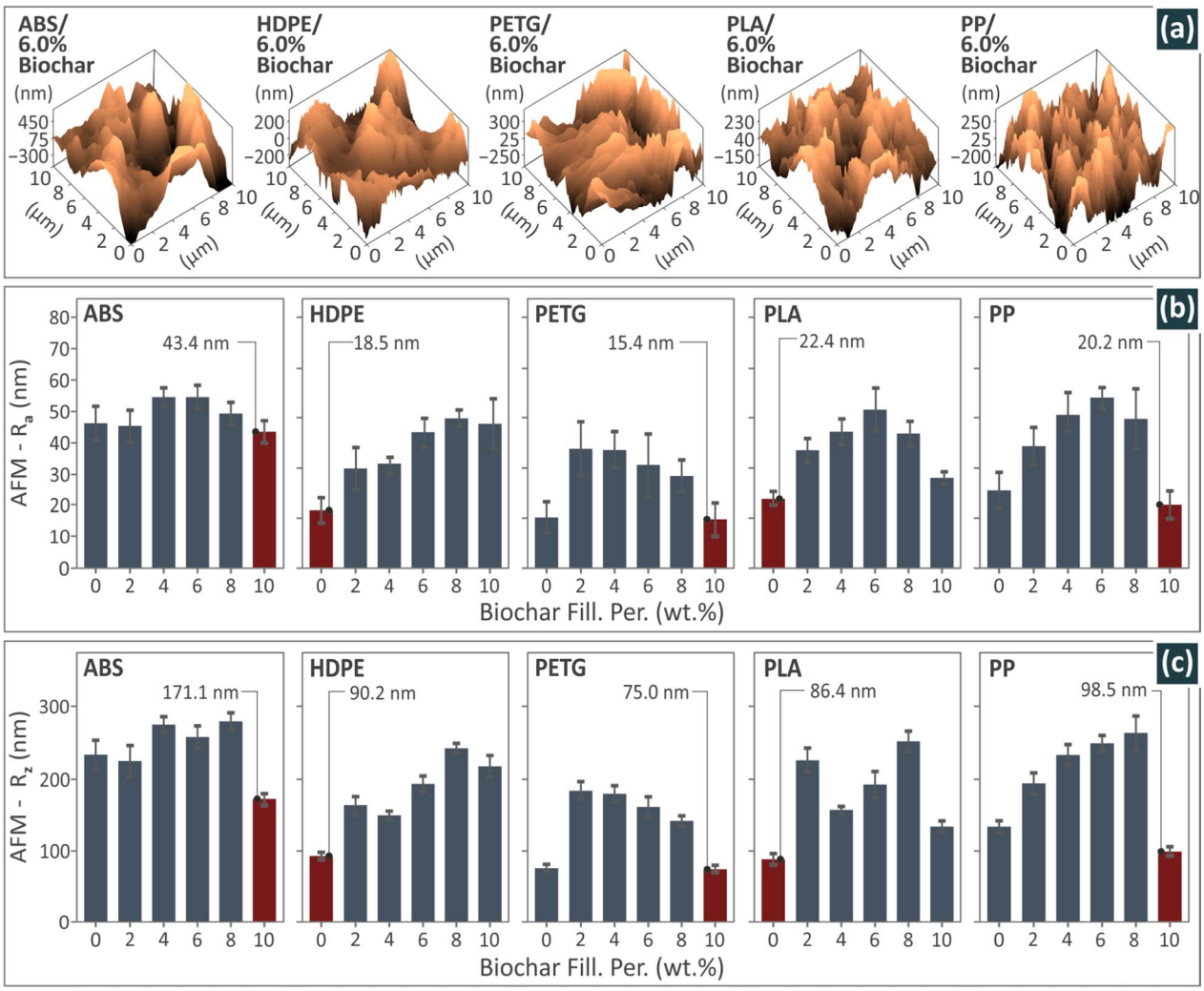

Fig. 4 AFM characterization of the filaments: **a** 3D height images showing the surface topology of ABS, HDPE, PETG, PP, and PLA/biochar 6.0 wt% filaments, **b** bars of the R_a metric mean values, and **c** R_z metric regarding all the ABS/biochar, HDPE/biochar, PETG/biochar, PLA/biochar, and PP/biochar filament composites of all the biochar percentages (0.0–10.0 wt%, with a 2.0 wt% step)

for the highest-loaded composite, whereas composites with lower concentrations showed higher surface roughness values.

3.2 CT scan characterization

Figure 5 shows the results from the CT scan, showing the deviation in the dimensions and porosity of the 3D-printed tensile specimens produced from ABS, HDPE, PETG, PP, and PLA/biochar 6.0 wt% composites. A virtual section from the material structure of the specimens was presented using color-coded technology. Specimens of polylactic acid (PLA and PP/biochar 6.0 wt% revealed dimensional deviation values mostly close to zero. However, a large proportion of ABS/biochar 6.0 wt% sample revealed values far from zero, which also happened in the case of HDPE and PETG/biochar samples, to a lesser extent. For the HDPE and PETG samples, the red-colored areas at the end of the samples indicate warping of the samples in these polymers, which are not present in the other three polymers. The respective color-coded images showing the distribution of the 3D-printed structure voids were shown at the bottom of each graph. The examination revealed pores with a small size that were almost uniformly distributed in the 3D-printed structure. Variations are evident between the materials, which can be attributed to the 3D-printed settings used and the differences in the flow response of the polymers due to the introduction of biochar particles, among other factors. The μ-CT findings were further analyzed and were presented below.

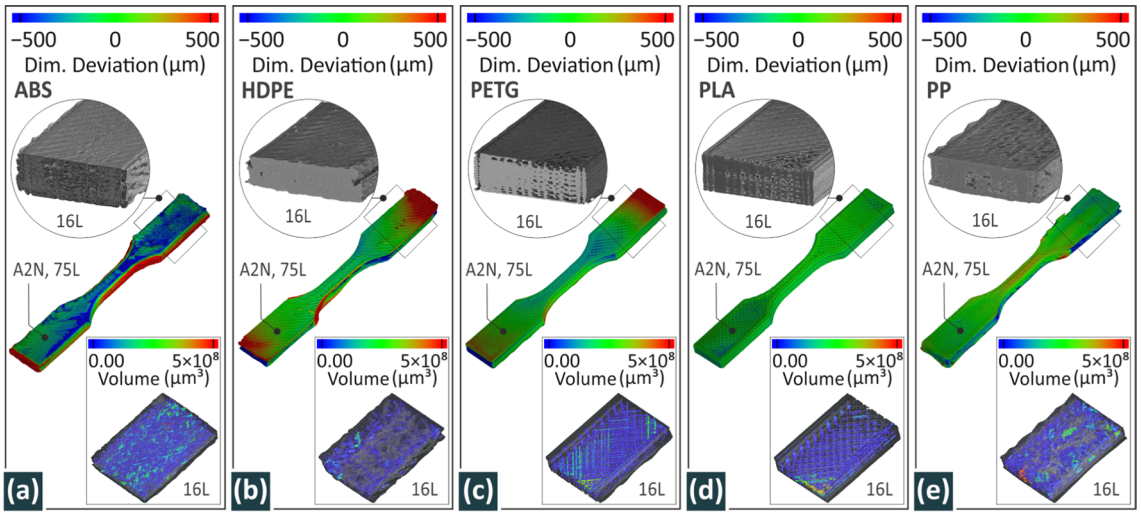

Fig. 5 CT-scan dimensional deviation of a randomly chosen tensile specimen from each composite tested **a** ABS/biochar, **b** HDPE/biochar, **c** PETG/biochar, **d** PLA/biochar and **e** PP/biochar, presenting a virtual section of the tensile specimens' material structure, through the color-coded technique

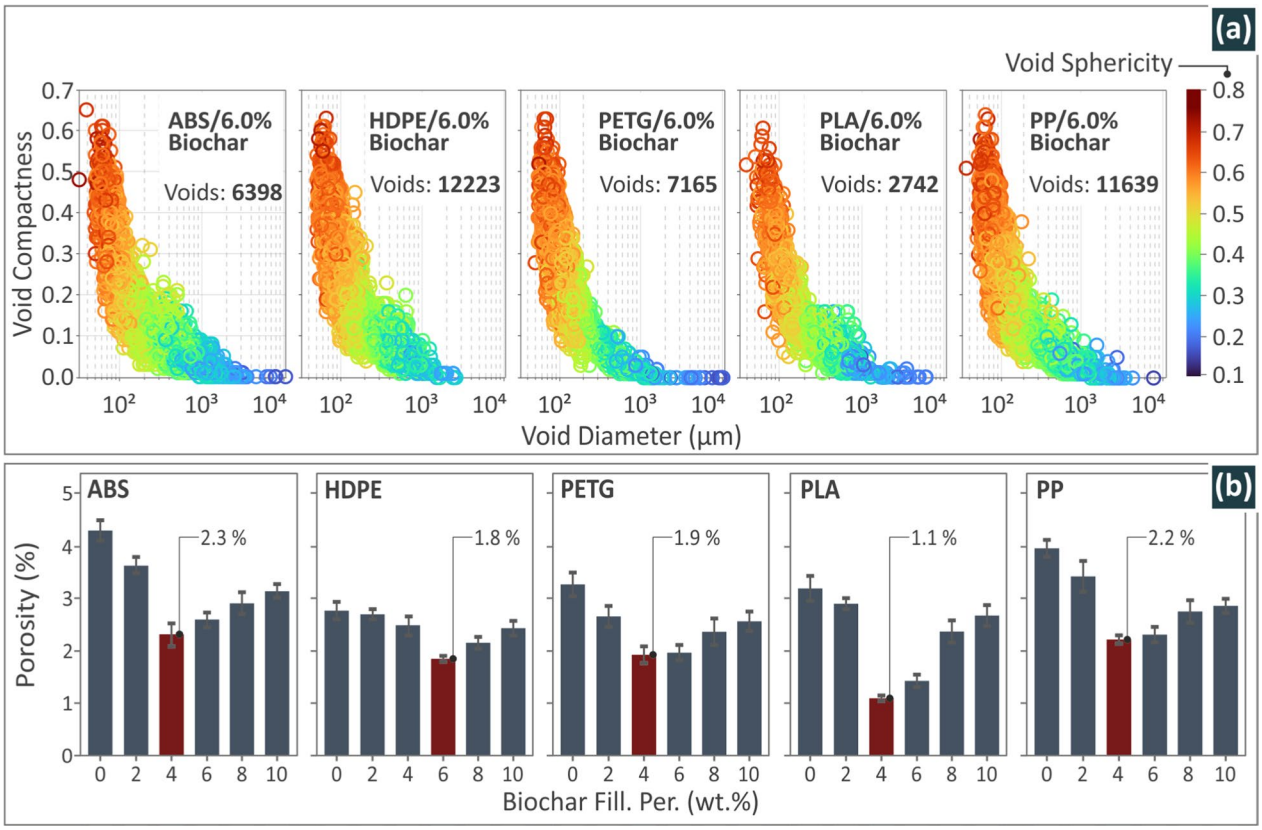

Fig. 6 Porosity characterization: **a** void compactness vs. diameter and void sphericity vs. diameter graphs for the ABS, HDPE, PETG, PP, and PLA/biochar 6.0 wt% composite samples, **b** bars of the average porosity values measured for all ABS, HDPE, PETG, PP, and PLA/biochar (0.0, 2.0, 4.0, 6.0, 8.0, and 10.0 wt%) composite samples, and highlight, in red, the best results observed for each case

3.3 Porosity characterization

In Fig. 6a, graphs of void compactness with respect to diameter and void sphericity with respect to diameter were created for ABS, HDPE, PETG, PP, and PLA/biochar 6.0 wt% composites. The HDPE and PP polymers presented the highest number of voids (12223 and 11639, respectively). Figure 6b shows the bars created by the mean porosity values of ABS, HDPE, PETG, PP, and PLA/biochar compounds. The compounds with HDPE as the matrix material and a biochar content of 6.0 wt% was the composite amongst all the HDPE/biochar composites that presented the lowest porosity. In ABS, PETG, PP, and PLA/biochar compounds, low levels were detected in the case of 4.0 wt%.

3.4 Dimensional deviation

Figure 7a shows graphs of the related surface and points to dimensional deviation for ABS, HDPE, PETG, PP, and PLA/biochar 6.0 wt% composites. Notably, PLA/biochar showed the greatest dimensional deviation, closer to zero. Figure 7b presents the A2N mean values of the ABS, HDPE, PETG, PP, and PLA/BC composites. For the ABS/BC and HDPE/BC composites, those of 6.0 wt% were the compound of the lowest dimensional deviation. The respective results for PETG were detected in the case of the 8.0 wt% composite, while for the PLA and PP, it was 4.0 wt%.

3.5 Optical profilometry results

Figure 8 shows the optical profilometry measurements of the composites investigated in this study. Figure 8a shows typical roughness maps of all compounds with a biochar content of 6.0 wt%. Figure 8b and c show the optical profilometry R_a and R_z mean values, respectively, for ABS, HDPE, PETG, PP, and PLA/biochar (0.0, 2.0, 4.0, 6.0, 8.0, and 10.0 wt%) composite samples. In the case of the ABS/biochar compounds, the 6.0 wt% and 10.0 wt% showed the smallest R_z and R_a roughness values detected, correspondingly. Regarding the HDPE/BC composites, the HDPE/biochar 0.0 wt% presented the smallest R_z and R_a roughness measurements. Additionally, the lowest values for the rest of the polymers were detected for PETG neat (Ra), PETG with 10.0 wt% biochar (Rz), PLA with

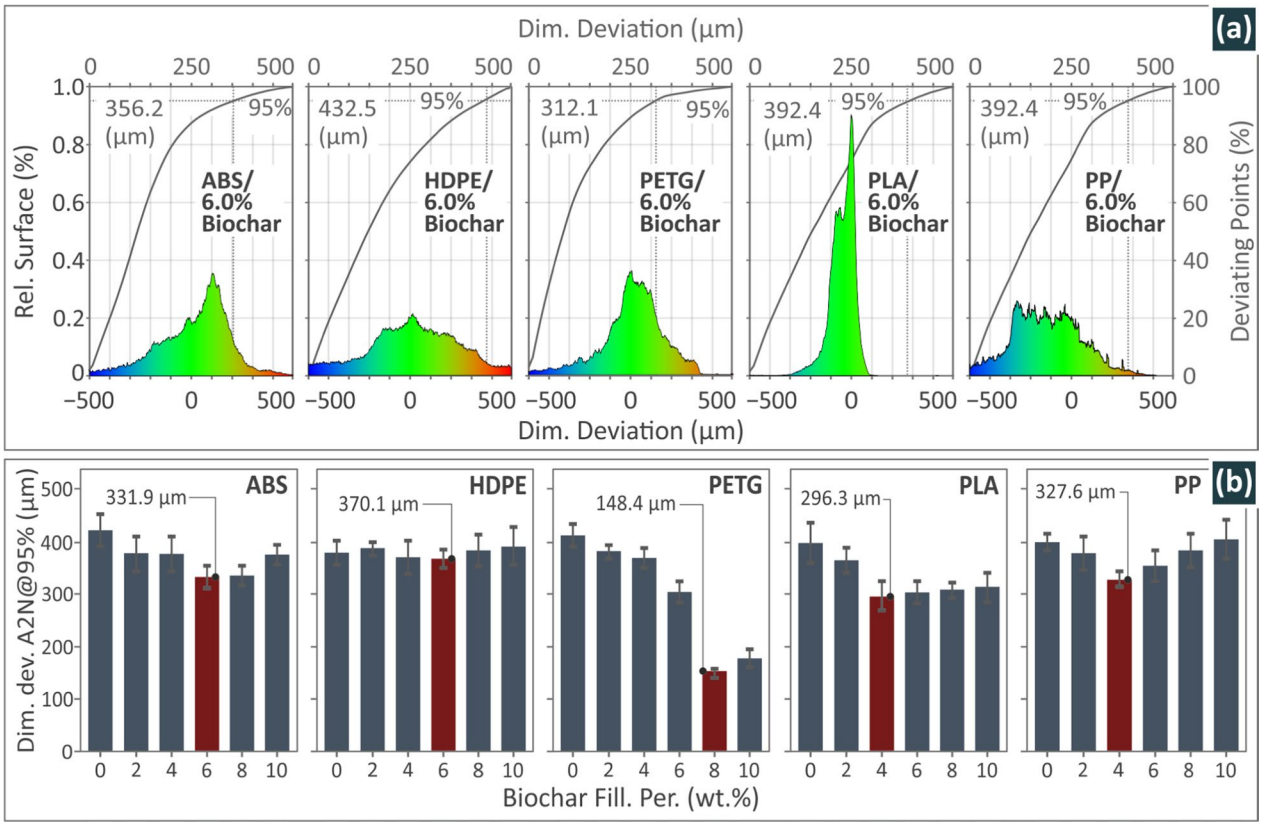

Fig. 7 A2N results: **a** related surface vs. dimensional deviation and deviating points vs. dimensional deviation graphs with regard to ABS, HDPE, PETG, PP, and PLA/biochar 6.0 wt% composite samples, **b** bars of the 95% values (5% of the most extreme values were disregarded) average A2N dimensional deviation, measured for all ABS, HDPE, PETG, PP, and PLA/biochar (0.0, 2.0, 4.0, 6.0, 8.0, and 10.0 wt%) composite samples, and highlight, in red, the best results observed for each case

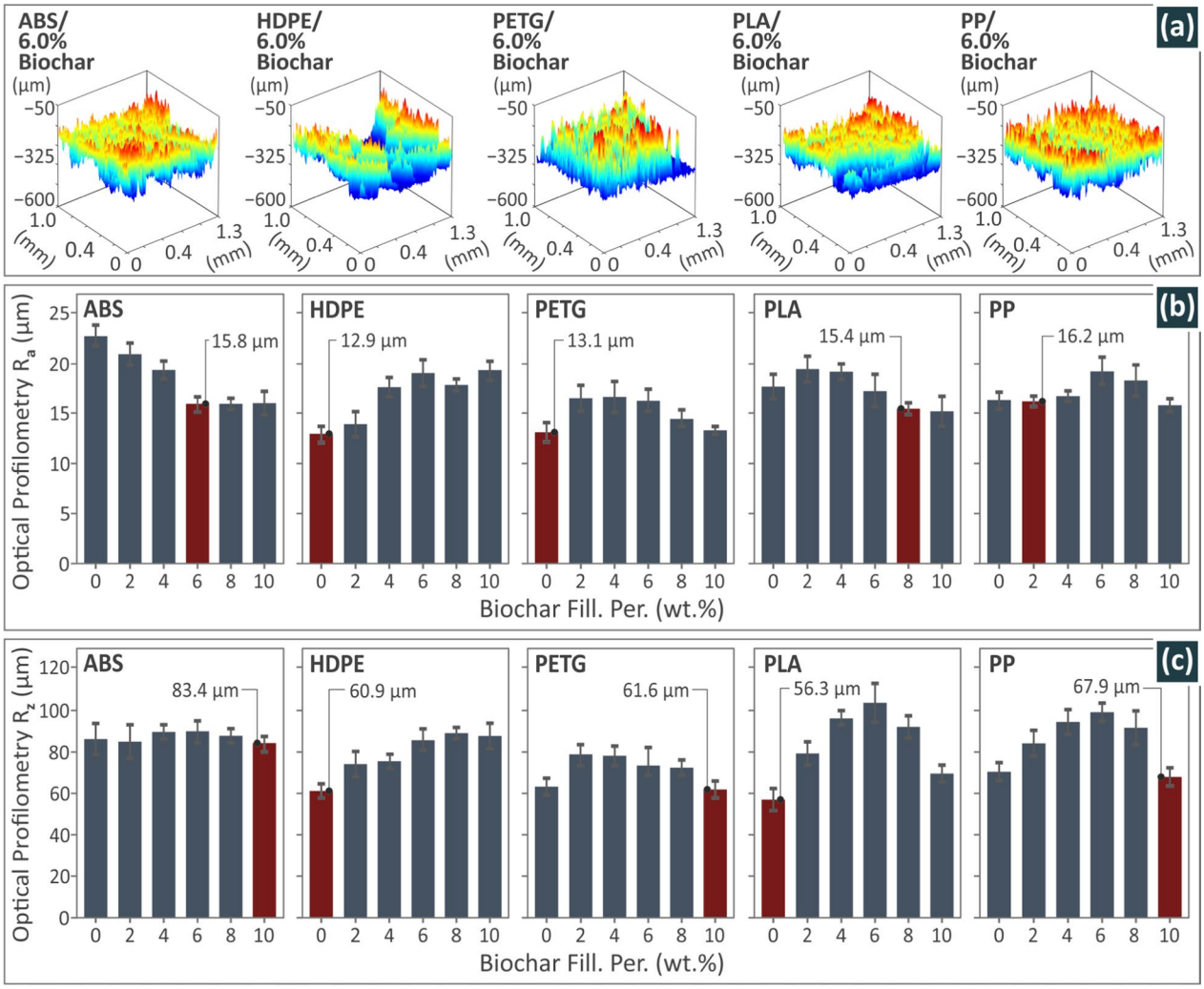

Fig. 8 Optical profilometry results: **a** typical roughness maps of the ABS, HDPE, PETG, PP, and PLA/biochar 6.0 wt% composite samples, **b** bars of the average surface roughness values Ra and **c** R_z, measured for all ABS, HDPE, PETG, PP, and PLA/biochar (0.0, 2.0, 4.0, 6.0, 8.0, and 10.0 wt%) composite samples, and highlight of the greatest results detected on each occasion

8.0 wt% biochar (Ra), PETG neat (Rz), PP with 2.0 wt% biochar (Ra) and PP with 10.0 wt% biochar (Rz).

3.6 Response results aggregation and analysis of parameters

In Fig. 9, the AFM R_a (Fig. 9a), AFM R_z (Fig. 9b), porosity (Fig. 9c), A2N (Fig. 9d), optical profilometry R_a (Fig. 9e), and optical profilometry R_z (Fig. 9f) values matched the corresponding σ_b measured values for all the ABS, HDPE, PETG, PP, and PLA/biochar composites. The calculated correlation coefficient, r, is presented for each quality metric and polymer. The results vary, with other metrics having positive values (strong correlation) and others having negative values (opposite correlation). The variation in these results highlights the necessity of this investigation and demonstrates the diverse effects of the different quality metrics of biochar particles and various polymeric materials. On the other hand, the calculated r values for each quality metric had the same sign for all polymers. The calculated r values were shown in the following Fig. 10.

In Fig. 10, the r values of all polymer/biochar composites derived from Fig. 9 are correlated. In particular, Fig. 10a and b present the correlation with R_a and R_z AFM values, Fig. 10c and d depict the porosity and A2N results, and Fig. 10e and f illustrate the optical profilometry R_a and R_z values, respectively. It can be observed that the A2N and porosity metrics present the greatest competitiveness. The porosity of PLA reached its lowest value, which also occurred in the case of A2N in PETG.

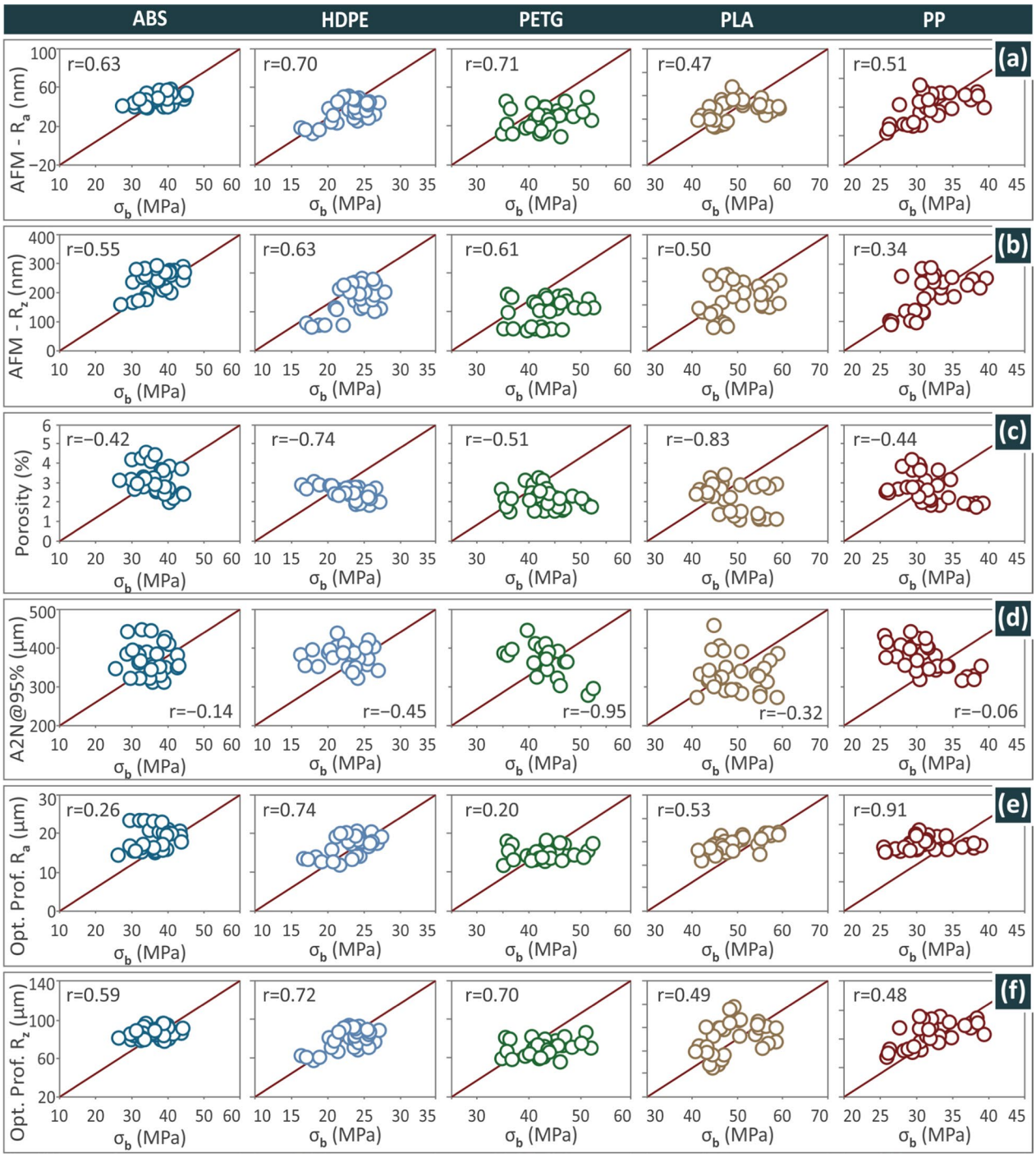

Fig. 9 Regarding all of the polymers (ABS, HDPE, PETG, PLA, and PP) investigated in the study herein: matching of the measured **a** AFM R_a, **b** AFM R_z, **c** porosity, **d** A2N, **e** optical profilometry R_a and **f** optical profilometry R_z values with the respective σ_b calculated values. The correlation coefficient for each metric is shown in the respective figure

The AFM R_a and R_z metrics were cooperative as they reached values over zero, which also occurred in the case of the optical profilometry R_a and R_z metrics. The polymers that revealed values closer to zero but still above it were PLA for AFM R_a and PP for AFM R_z, as well as ABS and PETG for optical profilometry R_a. It should be mentioned that the A2N values of ABS and PP were very close to zero. AFM Ra and Rz had positive r values, with the

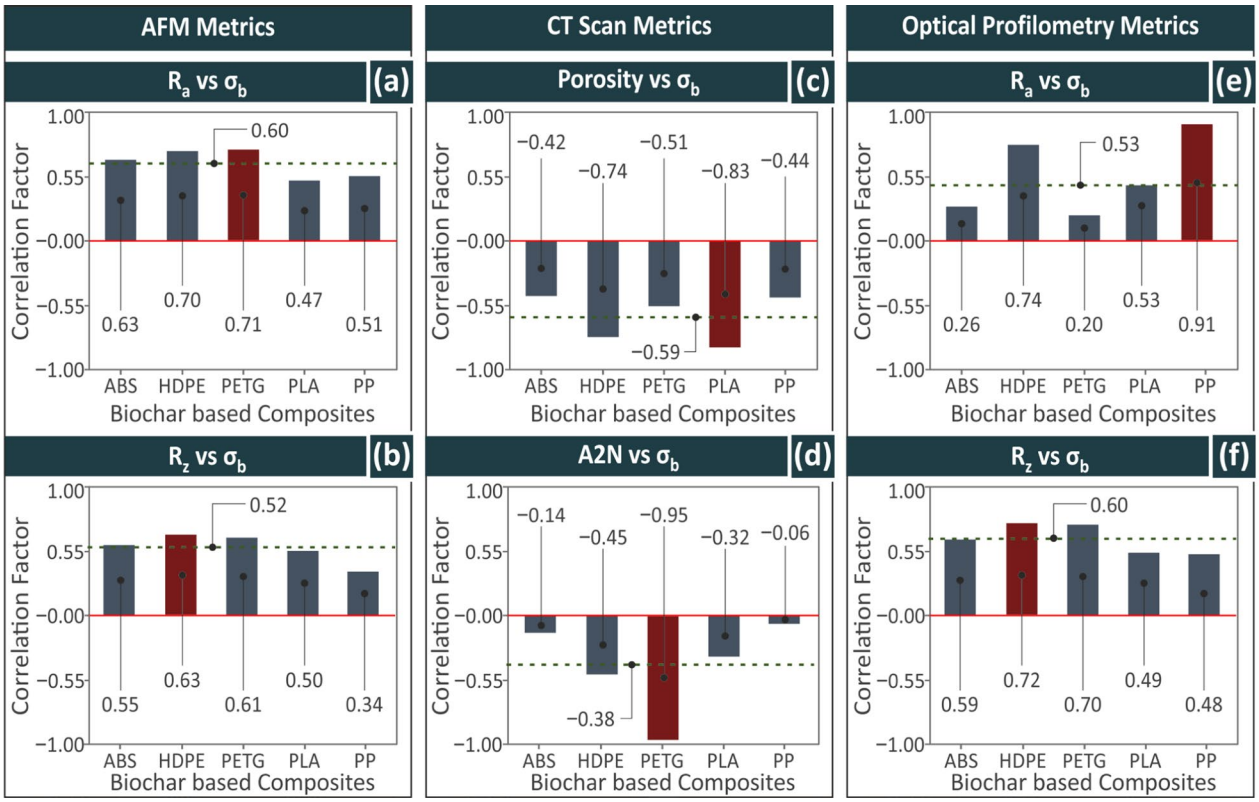

Fig. 10 Correlation of the **a** AFM R_a, **b** AFM R_z, **c** CT-scan porosity, **d** CT-scan A2N, **e** optical profilometry R_a and **f** optical profilometry R_z, versus σ_b results derived from the previous figure, of all of the polymeric materials (ABS, HDPE, PETG, PLA, and PP)

differences between the polymers being rather low. PETG and HDPE had the highest r values for Ra and Rz, respectively. Porosity and A2N both have negative r values for all polymers, indicating that an increase in porosity or dimensional deviation leads to samples with decreased tensile strength. The differences between the polymers in this case are significant, especially for the A2N metric, in which PETG has an r value close to −1, whereas ABS and PP are close to zero. Therefore, for these two polymers, A2N variation was not expected to significantly affect the tensile strength of the parts. For the porosity metric, the values between the polymers are not very different, with PLA having the highest r value in this case. The optical profilometry Ra and Rz measurements followed the same trend as the AFM measurements. However, in these measurements, the values showed higher differences. ABS and PETG had low r values for the Ra metric, whereas PP had a value close to 1. For the Rz metric, the differences between the polymers are smaller.

4 Discussion

In this study, five of the most frequently used MEX 3D printing polymers were chosen to create composites with biochar as an additive at six weight concentrations. Initially, mixtures were prepared and extruded into a form compatible with MEX 3D printing filaments. These were used to produce and characterize the respective samples, aiming to evaluate the differences in their quality characteristics and correlate them to their tensile strength (taken from the literature). According to the results, the filaments tested by AFM presented their lowest values of R_a and R_z roughness in the case of 0.0 wt% (no biochar present, for the HDPE, and PLA polymers) or in the case of 10.0 wt% (highest biochar content in the compounds tested, for the ABS, PETG, and PP polymers). Regarding porosity, the lowest values were obtained with 4.0 wt% in the case of ABS, PETG, PLA, and PP, as well as 6.0 wt% in the case of HDPE.

The quality metrics were correlated with the performance of the samples in the tensile experiment. The experimental results were obtained from the literature (ABS) (Vidakis et al. 2024d), HDPE (Vidakis et al. 2024e), PP (Petousis et al. 2024a), PLA (Vidakis et al. 2023b), which was expanded, and PETG, which has been studied but not yet published). In these studies, the reinforcement effect of biochar particles was analyzed and interpreted. The outcomes of the characterization process follow similar trends. For example, the melt flow index

(MFR) of polymers is reduced with the addition of biochar, and it is constantly reduced as the content of the particles increases. The reinforcement effect is higher for the HDPE polymer, among the five polymers, and lower for the PETG polymer, in which the improvement is approximately half of that of the HDPE. The compounds that achieved the highest tensile strength were 6 wt % biochar in the PETG and PP thermoplastics and 4 wt% on the remaining three polymers (ABS, PLA, HDPE). However, for the PETG and PP polymers, 4 wt% compounds showed high strength as well. Thus, the findings can be generalized for all polymers, with 4 wt% percentage being the optimum one.

As shown in Figs. 6 and 7, the introduction of biochar particles in the polymers initially, at lower biochar percentages, improved the porosity (lower percentage) and dimensional deviation (lower deviation). As the biochar content of the compounds increased, these two metrics worsened. However, the presence of biochar improved the porosity of the 3D-printed parts compared to that of the neat polymers. For all polymers, except HDPE, the lowest porosity was observed at 4 wt% biochar concentration, which had the highest tensile strength. HDPE, which had the highest improvement in its strength in the tensile experiment when biochar particles were added, had the highest number of voids, while PLA had the lowest number of voids. However, the porosity percentage in the HDPE thermoplastic was rather low among the five polymers, so the assumption that reduction of porosity contributes to higher mechanical strength stands here as well. Regarding the correlation coefficient, PLA had the highest (negative) r value, and ABS had the lowest value, about half that of PLA. Thus, PLA has a strong opposite correlation with the porosity metric. Fracture in the samples occurred as expected in a typical tensile test. A neck developed on the narrow part of the dogbone samples, and as the load increased, they failed. No surface delamination was observed. Interfacial interactions between the polymer and biochar were not investigated in this study. In this study, a laborious effort with six tests was carried out on biochar composites made with five different polymeric matrices at various concentrations. This study focuses on the effect of biochar on the quality metrics of different polymeric composites. Tensile tests were performed for completeness and to correlate the findings with the quality metrics. Interfacial interactions between the polymer and biochar can be included in future work.

Regarding geometric accuracy, HDPE showed the lowest values (the highest deviation among the five thermoplastics) because of the warping of the samples, which did not prevent it from having the highest reinforcement, as mentioned. Overall, the accuracy of the geometry had a similar effect on the differences in biochar content compounds and a similar effect on the five polymers. Only the PETG polymer showed a notable improvement in the geometrical accuracy (reduction of the dimensional deviation) for compounds with a higher biochar content. The actual to nominal correlation coefficient was almost −1 for the PETG polymer, while it was almost zero for the PP polymer, indicating large differences in the effect of the geometrical accuracy on the tensile strength between these two polymers.

The surface roughness of the samples, which is a quality metric related to the functionality of the samples, was measured using two different methods: AFM and optical profilometry. The values acquired using the two methods were similar and followed a similar trend. Differences were expected because of the randomly selected areas used for acquiring the measurements. However, the correlation between the values of the two methods and the tensile strength differs. The r values calculated for the Ra values measured with optical profilometry showed a low correlation for the ABS polymer, whereas the value for the PP was almost 1, showing a strong correlation. The respective values obtained with AFM, ABS, HDPE, and PETG had similar r values, and PLA and PP had lower r values (again close to each other). PP had the lowest r value (AFM measurements) for the Rz metric. These differences are not that high overall and can be attributed to the randomly selected areas for measurement using the two methods.

Herein, through a laborious effort with numerous measurements taken, an attempt was made to provide a complete analysis of the effect on four quality characteristics of the 3D-printed parts by the addition of biochar particles on five popular thermoplastics and a correlation with their tensile strength. In this study, testing was performed on 3D-printed samples manufactured with biochar composites developed within the context of the research. To ensure the replicability and reliability of the results, international standards were used for the mechanical and other tests. This is the standard scientific method commonly used in such studies. To determine the effect of biochar on the properties of the final items, the same procedure and standards were followed. Therefore, the results provided in the manuscript can also be safely applied to these items. A thermomechanical method was used to scale up the process, which was compatible with the MEX 3D printing process. The main advantage of this method is that it does not use any chemicals, and chemical reactions are not required to produce composites. Therefore, they can be easily scaled up for industrial applications. The MEX 3D-printed parts have already been tested within the context of this study. The literature review did not reveal any studies on the effect of biochar on

the quality characteristics of MEX 3D-printed examples. Therefore, the findings cannot be compared with similar studies from the literature, as the quality of the 3D-printed parts highly depends on the 3D printing process and the structure of the parts.

5 Conclusions

This study investigated eco-friendly biochar derived from olive pruning as an additive in composites made with five of the most popular polymeric matrices in MEX 3D printing, that is, ABS, PLA, HDPE, PETG, and PP, for its effect on the build quality of the parts. Composites for all polymers were prepared using the same method and biochar contents to obtain comparable results. The quality metrics studied were surface roughness, porosity, and geometrical accuracy. These were evaluated using AFM and optical profilometry for the R_z and R_a roughness metrics and μ-CT scanning for porosity and geometrical accuracy. The results obtained for the polymers were compared. Most importantly, the quality of the 3D-printed examples was correlated with their mechanical response in the tensile test by exploiting the results from the respective studies of this research group. The main findings were:

- The effects of the addition of biochar particles to the five polymers differed, justifying the need for such an analysis.
- Still, in all five polymeric matrices, the findings followed a similar trend.
- The quality metrics were correlated with the tensile strength of the composites using a correlation coefficient equation.
- Reduced porosity and better geometrical accuracy contributed to higher tensile strength.
- The 4 wt% composite in most polymers achieved better results in terms of quality and strength.

These results encourage further research into polymeric materials combined with biochar fillers, as well as exploring other filler percentages. The interfacial interactions between the polymer and biochar can be investigated, providing valuable information regarding the variations in the behavior of the different polymers studied. The 3D printing settings can be further optimized to achieve the highest mechanical performance. This can be done by considering the outcome of the characterization methods implemented, such as the rheology results because proper rheology of the material significantly affects the quality of the 3D-printed part. Finally, a study on the requirements for industrialization of the process can be carried out in future work.

Supplementary Information

The online version contains supplementary material available at https://doi.org/10.1007/s42773-024-00400-8.

Supplementary Material 1.

Acknowledgements
The authors would like to thank the Institute of Electronic Structure and Laser of the Foundation for Research and Technology-Hellas (IESL-FORTH) and, in particular, Ms. Aleka Manousaki for obtaining the SEM images presented in this study. We also express our gratitude to Evangelos Sotiropoulos from the Department of Electrical and Computer Engineering, Hellenic Mediterranean University (HMU), for conducting the AFM experiments.

Author contributions
Nectarios Vidakis: Conceptualization, methodology, resources, supervision, project administration; Markos Petousis: Methodology, writing—review, and editing; Dimitrios Sagris: Visualization, validation, data curation; Constantine David: Methodology, resources, project administration; Nikolaos Mountakis: Data curation and visualization; Mariza Spiridaki: Writing original draft, investigation; Emmanuel Maravelakis: Validation; Costas Charitidis: Writing — review and editing, supervision, validation; Emmanuel Stratakis: Methodology, resources, project administration. The manuscript was written with the contributions of all authors. All authors approved the final version of the manuscript.

Funding
This study did not receive any external funding.

Data availability
The raw/processed data required to reproduce these findings cannot be shared because of technical and time limitations.

Declarations

Competing interests
The authors have no competing interests to declare relevant to the content of this article.

Author details
[1]Department of Mechanical Engineering, Hellenic Mediterranean University, 71410 Heraklion, Greece. [2]Department of Mechanical Engineering, International Hellenic University, Serres Campus, 62124 Serres, Greece. [3]Department of Electronic Engineering, Hellenic Mediterranean University, 73133 Chania, Greece. [4]Department of Materials Science and Engineering, School of Chemical Engineering NTUA, National Technical University, Iroon Polytechneiou 9, 157 80 Zografou, Athens, Greece. [5]Foundation for Research and Technology-Hellas (FO.R.T.H), Heraklion, Crete, Greece. [6]Qingdao Innovation and Development Center, Harbin Engineering University, Qingdao, China.

Received: 10 August 2024 Revised: 30 October 2024 Accepted: 24 November 2024
Published online: 24 January 2025

References

Achilias DS, Roupakias C, Megalokonomos P, Lappas AA, Antonakou EV (2007) Chemical recycling of plastic wastes made from polyethylene (LDPE and HDPE) and polypropylene (PP). J Hazard Mater 149(3):536–542. https://doi.org/10.1016/j.jhazmat.2007.06.076

Afrose MF, Masood SH, Iovenitti P, Nikzad M, Sbarski I (2016) Effects of part build orientations on fatigue behaviour of FDM-processed PLA material. Progress Additive Manuf 1(1–2):21–28. https://doi.org/10.1007/s40964-015-0002-3

Ahmetli G, Kocaman S, Ozaytekin I, Bozkurt P (2013) Epoxy composites based on inexpensive char filler obtained from plastic waste and natural

resources. Polym Compos 34(4):500–509. https://doi.org/10.1002/pc.22452
Akhtar A, Sarmah AK (2018) Novel biochar-concrete composites: manufacturing, characterization and evaluation of the mechanical properties. Sci Total Environ 616–617:408–416. https://doi.org/10.1016/j.scitotenv.2017.10.319
Alauddin M, Choudhury IA, El Baradie MA, Hashmi MSJ (1995) Plastics and their machining: a review. J Mater Process Technol 54(1–4):40–46. https://doi.org/10.1016/0924-0136(95)01917-0
Almuallim B, Harun WSW, Al Rikabi IJ, Mohammed HA (2022) Thermally conductive polymer nanocomposites for filament-based additive manufacturing. J Mater Sci 57(6):3993–4019. https://doi.org/10.1007/s10853-021-06820-2
Andersen L, Wejdling A, Neidel T (2015) Plastic Waste–background report. Nordic Council of Ministers, Beau Vallon, Seychelles
Anerao P, Kulkarni A, Munde Y, Shinde A, Das O (2023) Biochar reinforced PLA composite for fused deposition modelling (FDM): a parametric study on mechanical performance. Compos Part C Open Access 12:100406. https://doi.org/10.1016/j.jcomc.2023.100406
Asuero AG, Sayago A, González AG (2006) The correlation coefficient: an overview. Crit Rev Anal Chem 36(1):41–59. https://doi.org/10.1080/10408340500526766
Auras R, Harte B, Selke S (2004) An overview of polylactides as packaging materials. Macromol Biosci 4(9):835–864. https://doi.org/10.1002/mabi.200400043
Autoeuropa V (2017) Maximizing production efficiency with 3D printed tools, jigs, and fixtures. Ultimaker, Utrecht
Badia JD, Strömberg E, Karlsson S, Ribes-Greus A (2012) The role of crystalline, mobile amorphous and rigid amorphous fractions in the performance of recycled poly (ethylene terephthalate) (PET). Polym Degrad Stab 97(1):98–107. https://doi.org/10.1016/j.polymdegradstab.2011.10.008
Bałdowska-Witos P, Kruszelnicka W, Tomporowski A (2020) Life cycle assessment of beverage bottles. J Phys Conf Ser 1426(1):012038. https://doi.org/10.1088/1742-6596/1426/1/012038
Bichu YM, Alwafi A, Liu X, Andrews J, Ludwig B, Bichu AY, Zou B (2023) Advances in orthodontic clear aligner materials. Bioact Mater 22:384–403. https://doi.org/10.1016/j.bioactmat.2022.10.006
Carneiro OS, Silva AF, Gomes R (2015) Fused deposition modeling with polypropylene. Mater Des 83:768–776. https://doi.org/10.1016/j.matdes.2015.06.053
Chacón JM, Caminero MA, García-Plaza E, Núñez PJ (2017) Additive manufacturing of PLA structures using fused deposition modelling: Effect of process parameters on mechanical properties and their optimal selection. Mater Des 124:143–157. https://doi.org/10.1016/j.matdes.2017.03.065
Chen L, Zhang Y, Wang L, Ruan S, Chen J, Li H, Yang J, Mechtcherine V, Tsang DCW (2022) Biochar-augmented carbon-negative concrete. Chem Eng J 431:133946. https://doi.org/10.1016/j.cej.2021.133946
Cosentino I, Restuccia L, Ferro GA, Tulliani J-M (2019) Type of materials, pyrolysis conditions, carbon content and size dimensions: the parameters that influence the mechanical properties of biochar cement-based composites. Theoret Appl Fract Mech 103:102261. https://doi.org/10.1016/j.tafmec.2019.102261
Couture A, Lebrun G, Laperrière L (2016) Mechanical properties of polylactic acid (PLA) composites reinforced with unidirectional flax and flax-paper layers. Compos Struct 154:286–295. https://doi.org/10.1016/j.compstruct.2016.07.069
Das O, Sarmah AK, Bhattacharyya D (2015) A novel approach in organic waste utilization through biochar addition in wood/polypropylene composites. Waste Manag 38:132–140. https://doi.org/10.1016/j.wasman.2015.01.015
Das C, Tamrakar S, Kiziltas A, Xie X (2021) Incorporation of Biochar to Improve Mechanical, Thermal and Electrical properties of Polymer composites. Polym (Basel) 13(16):2663. https://doi.org/10.3390/polym13162663
Dhakal N, Wang X, Espejo C, Morina A, Emami N (2023) Impact of processing defects on microstructure, surface quality, and tribological performance in 3D printed polymers. J Mater Res Technol 23:1252–1272. https://doi.org/10.1016/j.jmrt.2023.01.086
Drumright RE, Gruber PR, Henton DE (2000) Polylactic acid technology. Adv Mater 12(23):1841–1846.
Dupaix RB, Boyce MC (2005) Finite strain behavior of poly(ethylene terephthalate) (PET) and poly(ethylene terephthalate)-glycol (PETG). Polym (Guildf) 46(13):4827–4838. https://doi.org/10.1016/j.polymer.2005.03.083
Durgashyam K, Indra Reddy M, Balakrishna A, Satyanarayana K (2019) Experimental investigation on mechanical properties of PETG material processed by fused deposition modeling method. Mater Today Proc 18:2052–2059. https://doi.org/10.1016/j.matpr.2019.06.082
Dusunceli N, Colak OU (2008) The effects of manufacturing techniques on viscoelastic and viscoplastic behavior of high density polyethylene (HDPE). Mater Des 29(6):1117–1124. https://doi.org/10.1016/j.matdes.2007.06.003
Elfaleh I, Abbassi F, Habibi M, Ahmad F, Guedri M, Nasri M, Garnier C (2023) A comprehensive review of natural fibers and their composites: an eco-friendly alternative to conventional materials. Results Eng 19:101271. https://doi.org/10.1016/j.rineng.2023.101271
Falliano D, De Domenico D, Quattrocchi S, Cosenza P, Ricciardi G, Restuccia L, Ferro GA (2020) Mechanical properties and carbon footprint of 3D-printable cement mortars with biochar additions. MATEC Web Conf 323:01017. https://doi.org/10.1051/matecconf/202032301017
George J, Jung D, Bhattacharyya D (2023) Improvement of electrical and mechanical properties of PLA/PBAT composites using coconut shell biochar for antistatic applications. Appl Sci 13(2):902. https://doi.org/10.3390/app13020902
Geyer R, Jambeck JR, Law KL (2017) Production, use, and fate of all plastics ever made. Sci Adv. https://doi.org/10.1126/sciadv.1700782
Giorcelli M, Khan A, Pugno NM, Rosso C, Tagliaferro A (2019) Biochar as a cheap and environmental friendly filler able to improve polymer mechanical properties. Biomass Bioenergy 120:219–223. https://doi.org/10.1016/j.biombioe.2018.11.036
Guessasma S, Belhabib S, Nouri H (2019) Printability and Tensile performance of 3D printed polyethylene terephthalate glycol using fused deposition modelling. Polym (Basel) 11(7):1220. https://doi.org/10.3390/polym11071220
Gupta B, Revagade N, Hilborn J (2007) Poly(lactic acid) fiber: an overview. Prog Polym Sci 32(4):455–482. https://doi.org/10.1016/j.progpolymsci.2007.01.005
Habel C, Schöttle M, Daab M, Eichstaedt NJ, Wagner D, Bakhshi H, Agarwal S, Horn MA, Breu J (2018) High-barrier, biodegradable food packaging. Macromol Mater Eng. https://doi.org/10.1002/mame.201800333
Hagemann N, Joseph S, Schmidt H-P, Kammann CI, Harter J, Borch T, Young RB, Varga K, Taherymoosavi S, Elliott KW, McKenna A, Albu M, Mayrhofer C, Obst M, Conte P, Dieguez-Alonso A, Orsetti S, Subdiaga E, Behrens S, Kappler A (2017) Organic coating on biochar explains its nutrient retention and stimulation of soil fertility. Nat Commun 8(1):1089. https://doi.org/10.1038/s41467-017-01123-0
He M, Xu Z, Hou D, Gao B, Cao X, Ok YS, Rinklebe J, Bolan NS, Tsang DCW (2022) Waste-derived biochar for water pollution control and sustainable development. Nat Rev Earth Environ 3(7):444–460. https://doi.org/10.1038/s43017-022-00306-8
Ho M, Lau K, Wang H, Hui D (2015) Improvement on the properties of polylactic acid (PLA) using bamboo charcoal particles. Compos B Eng 81:14–25. https://doi.org/10.1016/j.compositesb.2015.05.048
Hussain T, Tausif M, Ashraf M (2015) A review of progress in the dyeing of eco-friendly aliphatic polyester-based polylactic acid fabrics. J Clean Prod 108:476–483. https://doi.org/10.1016/j.jclepro.2015.05.126
Idrees M, Jeelani S, Rangari V (2018) Three-dimensional-printed sustainable Biochar-recycled PET composites. ACS Sustain Chem Eng 6(11):13940–13948. https://doi.org/10.1021/acssuschemeng.8b02283
Insight ace analytic (2024) Global biochar research report. In: https://www.insightaceanalytic.com/report/biochar-market/2094#:~:text=Biochar%20Market%20Size%20is%20valued,forecast%20period%20for%202023%2D2031
Jayakumar A, Morrisset D, Koutsomarkos V, Wurzer C, Hadden RM, Lawton L, Edwards C, Mašek O (2023) Systematic evaluation of pyrolysis processes and biochar quality in the operation of low-cost flame curtain pyrolysis kiln for sustainable biochar production. Curr Res Environ Sustain 5:100213. https://doi.org/10.1016/j.crsust.2023.100213
Joseph PV, Rabello MS, Mattoso LHC, Joseph K, Thomas S (2002) Environmental effects on the degradation behaviour of sisal fibre reinforced

polypropylene composites. Compos Sci Technol 62(10–11):1357–1372. https://doi.org/10.1016/S0266-3538(02)00080-5
Kalsoom U, Peristyy A, Nesterenko PN, Paull B (2016) A 3D printable diamond polymer composite: a novel material for fabrication of low cost thermally conducting devices. RSC Adv 6(44):38140–38147. https://doi.org/10.1039/C6RA05261D
Laureto JJ, Pearce JM (2018) Anisotropic mechanical property variance between ASTM D638-14 type i and type iv fused filament fabricated specimens. Polym Test 68:294–301. https://doi.org/10.1016/j.polymertesting.2018.04.029
Lee BH, Abdullah J, Khan ZA (2005) Optimization of rapid prototyping parameters for production of flexible ABS object. J Mater Process Technol 169(1):54–61. https://doi.org/10.1016/j.jmatprotec.2005.02.259
Lee Rodgers J, Nicewander WA (1988) Thirteen ways to look at the correlation coefficient. Am Stat 42(1):59–66. https://doi.org/10.1080/00031305.1988.10475524
Leng L, Huang H (2018) An overview of the effect of pyrolysis process parameters on biochar stability. Bioresour Technol 270:627–642. https://doi.org/10.1016/j.biortech.2018.09.030
Li B, Zhang X, Zhang Q, Chen F, Fu Q (2009) Synergistic enhancement in tensile strength and ductility of ABS by using recycled PETG plastic. J Appl Polym Sci 113(2):1207–1215. https://doi.org/10.1002/app.30002
Li S, Xu Y, Jing X, Yilmaz G, Li D, Turng L-S (2020) Effect of carbonization temperature on mechanical properties and biocompatibility of biochar/ultra-high molecular weight polyethylene composites. Compos B Eng 196:108120. https://doi.org/10.1016/j.compositesb.2020.108120
Lukkassen D, Meidell A (2003) Advanced materials and structures and their fabrication processes. Narrik University College, Hin
Musa ET, Hamza A, Ahmed AS, Ishiuku US (2017) Investigation of the mechanical and morphological properties of high-density polyethylene (Hdpe)/leather waste composites. IOSR J Appl Chem 10(01):48–58. https://doi.org/10.9790/5736-1001014858
Maljaee H, Madadi R, Paiva H, Tarelho L, Ferreira VM (2021) Incorporation of biochar in cementitious materials: a roadmap of biochar selection. Constr Build Mater 283:122757. https://doi.org/10.1016/j.conbuildmat.2021.122757
Mayakrishnan V, Mohamed JK, Selvaraj N, SenthilKumar D, Annadurai S (2023) Effect of nano-biochar on mechanical, barrier and mulching properties of 3D printed thermoplastic polyurethane film. Polym Bull 80(6):6725–6747. https://doi.org/10.1007/s00289-022-04380-2
Michailidis N, Petousis M, Moutsopoulou A, Argyros A, Ntintakis I, Papadakis V, Nasikas NK, Vidakis N (2024) Engineering response of biomedical grade isotactic polypropylene reinforced with titanium nitride nanoparticles for material extrusion three-dimensional printing. Eur J Mater 4(1):1–24. https://doi.org/10.1080/26889277.2024.2340944
Miller AT, Safranski DL, Smith KE, Sycks DG, Guldberg RE, Gall K (2017) Fatigue of injection molded and 3D printed polycarbonate urethane in solution. Polym (Guildf) 108:121–134. https://doi.org/10.1016/j.polymer.2016.11.055
Minugu OP, Gujjala R, Shakuntala O, Manoj P, Chowdary MS (2021) Effect of biomass derived biochar materials on mechanical properties of biochar epoxy composites. Proc Inst Mech Eng C J Mech Eng Sci 235(21):5626–5638. https://doi.org/10.1177/0954406221990705
Mohamed OA, Masood SH, Bhowmik JL (2016) Experimental investigation of the influence of fabrication conditions on dynamic viscoelastic properties of PC-ABS processed parts by FDM process. IOP Conf Ser Mater Sci Eng 149:012122. https://doi.org/10.1088/1757-899X/149/1/012122
Murariu M, Dubois P (2016) PLA composites: from production to properties. Adv Drug Deliv Rev 107:17–46. https://doi.org/10.1016/j.addr.2016.04.003
Nasikas NK, Petousis M, Papadakis V, Argyros A, Valsamos J, Gkagkanatsiou K, Sagris D, David C, Michailidis N, Maravelakis E, Vidakis N (2024) **A** comprehensive optimization course of antimony tin oxide nanofiller loading in polyamide 12: printability, quality assessment, and engineering response in additive manufacturing. Nanomaterials. https://doi.org/10.3390/nano14151285
Ngo TD, Kashani A, Imbalzano G, Nguyen KTQ, Hui D (2018) Additive manufacturing (3D printing): a review of materials, methods, applications and challenges. Compos B Eng 143:172–196. https://doi.org/10.1016/j.compositesb.2018.02.012
Nikolopoulos CD, Baklezos AT, Kapetanakis TN, Vardiambasis IO, Tsubota T, Kalderis D (2023) Characterization of the electromagnetic shielding effectiveness of biochar-based materials. IEEE Access 11:6413–6420. https://doi.org/10.1109/ACCESS.2023.3237327
Nikzad M, Masood SH, Sbarski I (2011) Thermo-mechanical properties of a highly filled polymeric composites for fused deposition modeling. Mater Des 32(6):3448–3456. https://doi.org/10.1016/j.matdes.2011.01.056
Paszkiewicz S, Szymczyk A, Pawlikowska D, Irska I, Taraghi I, Pilawka R, Gu J, Li X, Tu Y, Piesowicz E (2017) Synthesis and characterization of poly(ethylene terephthalate-co-1,4-cyclohexanedimethylene terephtlatate)-block-poly(tetramethylene oxide) copolymers. RSC Adv 7(66):41745–41754. https://doi.org/10.1039/C7RA07172H
Pearson K, Galton F (1997) VII. Note on regression and inheritance in the case of two parents. Proc Royal Soc London 58(347–352):240–42. https://doi.org/10.1098/rspl.1895.0041
Pervaiz M, Sain MM (2003) Sheet-molded polyolefin natural fiber composites for automotive applications. Macromol Mater Eng 288(7):553–557. https://doi.org/10.1002/mame.200350002
Petousis M, Maravelakis E, Kalderis D, Saltas V, Mountakis N, Spiridaki M, Bolanakis N, Argyros A, Papadakis V, Michailidis N, Vidakis N (2024a) Biochar for sustainable additive manufacturing: Thermal, mechanical, electrical, and rheological responses of polypropylene-biochar composites. Biomass Bioenergy 186:107272. https://doi.org/10.1016/j.biombioe.2024.107272
Petousis M, Michailidis N, Saltas V, Papadakis V, Spiridaki M, Mountakis N, Argyros A, Valsamos J, Nasikas NK, Vidakis N (2024b) Mechanical and electrical properties of polyethylene terephthalate glycol/antimony tin oxide nanocomposites in material extrusion 3D printing. Nanomaterials 14(9):761. https://doi.org/10.3390/nano14090761
Petousis M, Sagris D, Papadakis V, Moutsopoulou A, Argyros A, David C, Valsamos J, Spiridaki M, Michailidis N, Vidakis N (2024c) Optimization course of titanium nitride nanofiller loading in high-density polyethylene: interpretation of reinforcement effects and performance in material extrusion 3D printing. Polym (Basel). https://doi.org/10.3390/polym16121702
Petrov P, Agzamova D, Pustovalov V, Zhikhareva E, Saprykin B, Chmutin I, Shmakova N (2021) Research into the effect of the 3D-printing mode on changing the properties of PETG transparent plastic. ESAFORM. https://doi.org/10.25518/esaform21.3763
Postiglione G, Natale G, Griffini G, Levi M, Turri S (2015) Conductive 3D microstructures by direct 3D printing of polymer/carbon nanotube nanocomposites via liquid deposition modeling. Compos Part Appl Sci Manuf 76:110–114. https://doi.org/10.1016/j.compositesa.2015.05.014
Rasal RM, Janorkar AV, Hirt DE (2010) Poly(lactic acid) modifications. Prog Polym Sci 35(3):338–356. https://doi.org/10.1016/j.progpolymsci.2009.12.003
Sain M, Suhara P, Law S, Bouilloux A (2005) Interface modification and mechanical properties of natural fiber-polyolefin composite products. J Reinf Plast Compos 24(2):121–130. https://doi.org/10.1177/0731684405041717
Sajjadi B, Chen W-Y, Egiebor NO (2019) A comprehensive review on physical activation of biochar for energy and environmental applications. Rev Chem Eng 35(6):735–776. https://doi.org/10.1515/revce-2017-0113
Sawyer DJ (2003) Bioprocessing – no longer a field of dreams. Macromol Symp 201(1):271–282. https://doi.org/10.1002/masy.200351130
Sedgwick P (2012) Pearson's correlation coefficient. BMJ Br Med J 345:e4483. https://doi.org/10.1136/bmj.e4483
Serra T, Planell JA, Navarro M (2013) High-resolution PLA-based composite scaffolds via 3-D printing technology. Acta Biomater 9(3):5521–5530. https://doi.org/10.1016/j.actbio.2012.10.041
Shanmugam V, Sreenivasan SN, Mensah RA, Försth M, Sas G, Hedenqvist MS, Neisiany RE, Tu Y, Das O (2022) A review on combustion and mechanical behaviour of pyrolysis biochar. Mater Today Commun 31:103629. https://doi.org/10.1016/j.mtcomm.2022.103629
Shubhra QTH, Alam AKMM, Beg MDH, Khan MA, Gafur MA (2011) Mechanical and degradation characteristics of natural silk and synthetic phosphate glass fiber reinforced polypropylene composites. J Compos Mater 45(12):1305–1313. https://doi.org/10.1177/0021998310380290

Shubhra QT, Alam A, Quaiyyum M (2013) Mechanical properties of polypropylene composites. J Thermoplast Compos Mater 26(3):362–391. https://doi.org/10.1177/0892705711428659
Snowdon MR, Mohanty AK, Misra M (2014) A study of carbonized lignin as an alternative to carbon black. ACS Sustain Chem Eng 2(5):1257–1263. https://doi.org/10.1021/sc500086v
Somani RH, Yang L, Sics I, Hsiao BS, Pogodina NV, Winter HH, Agarwal P, Fruitwala H, Tsou A (2002) Orientation-induced crystallization in isotactic polypropylene melt by shear deformation. Macromol Symp 185(1):105–117.
Szykiedans K, Credo W, Osiński D (2017) Selected mechanical properties of PETG 3-D prints. Procedia Eng 177:455–461. https://doi.org/10.1016/j.proeng.2017.02.245
Taib N-AAB, Rahman MR, Huda D, Kuok KK, Hamdan S, Bakri MK, Bin, Julaihi MRM, Bin, Khan A (2023) A review on poly lactic acid (PLA) as a biodegradable polymer. Polym Bull 80(2):1179–1213. https://doi.org/10.1007/s00289-022-04160-y
Tekinalp HL, Kunc V, Velez-Garcia GM, Duty CE, Love LJ, Naskar AK, Blue CA, Ozcan S (2014) Highly oriented carbon fiber–polymer composites via additive manufacturing. Compos Sci Technol 105:144–150. https://doi.org/10.1016/j.compscitech.2014.10.009
Tian X, Liu T, Yang C, Wang Q, Li D (2016) Interface and performance of 3D printed continuous carbon fiber reinforced PLA composites. Compos Part Appl Sci Manuf 88:198–205. https://doi.org/10.1016/j.compositesa.2016.05.032
Torrado Perez AR, Roberson DA, Wicker RB (2014) Fracture surface analysis of 3D-Printed tensile specimens of novel ABS-Based materials. J Fail Anal Prev 14(3):343–353. https://doi.org/10.1007/s11668-014-9803-9
Tsubota T, Tsuchiya S, Kusumoto T, Kalderis D (2021) Assessment of Biochar produced by Flame-Curtain Pyrolysis as a Precursor for the development of an efficient Electric double-layer Capacitor. Energies (Basel) 14(22):7671. https://doi.org/10.3390/en14227671
Vidakis N, David C, Petousis M, Sagris D, Mountakis N (2023a) Optimization of key quality indicators in material extrusion 3D printing of acrylonitrile butadiene styrene: the impact of critical process control parameters on the surface roughness, dimensional accuracy, and porosity. Mater Today Commun. https://doi.org/10.1016/j.mtcomm.2022.105171
Vidakis N, Kalderis D, Petousis M, Maravelakis E, Mountakis N, Bolanakis N, Papadakis V (2023b) Biochar filler in MEX and VPP additive manufacturing: characterization and reinforcement effects in polylactic acid and standard grade resin matrices. Biochar 5(1):39. https://doi.org/10.1007/s42773-023-00238-6
Vidakis N, Moutsopoulou A, Petousis M, Michailidis N, Charou C, Papadakis V, Mountakis N, Dimitriou E, Argyros A (2023c) Rheology and thermomechanical evaluation of additively manufactured acrylonitrile butadiene styrene (ABS) with optimized tungsten carbide (WC) nano-ceramic content. Ceram Int. https://doi.org/10.1016/j.ceramint.2023.08.144
Vidakis N, Petousis M, Michailidis N, Mountakis N, Argyros A, Spiridaki M, Moutsopoulou A, Papadakis V, Charitidis C (2023d) High-density polyethylene/carbon black composites in material extrusion additive manufacturing: conductivity, thermal, rheological, and mechanical responses. Polymers (Basel) 15:4717
Vidakis N, Petousis M, Michailidis N, Nasikas N, Papadakis V, Argyros A, Mountakis N, Charou C, Moutsopoulou A (2023e) Optimizing Titanium Carbide (TiC) ceramic nanofiller loading in isotactic polypropylene for MEX additive manufacturing: mechano-thermal and rheology aspects. Mater Today Commun. https://doi.org/10.1016/j.mtcomm.2023.107368
Vidakis N, Kalderis D, Michailidis N, Papadakis V, Mountakis N, Argyros A, Spiridaki M, Moutsopoulou A, Petousis M (2024a) Environmentally friendly polylactic acid/ferronickel slag composite filaments for material extrusion 3D printing: a comprehensive optimization of the filler content. Mater Today Sustain. https://doi.org/10.1016/j.mtsust.2024.100881
Vidakis N, Michailidis N, Petousis M, Nasikas NK, Saltas V, Papadakis V, Mountakis N, Argyros A, Spiridaki M, Valsamos I (2024b) Multifunctional HDPE/Cu biocidal nanocomposites for MEX additive manufactured parts: perspectives for the defense industry. Def Technol. https://doi.org/10.1016/j.dt.2024.03.004
Vidakis N, Petousis M, David C, Nasikas NK, Sagris D, Mountakis N, Spiridaki M, Moutsopoulou A, Stratakis E (2024c) Critical quality indicators of high-performance polyetherimide (ULTEM) over the MEX 3D printing key generic control parameters: prospects for personalized equipment in the defense industry. Def Technol. https://doi.org/10.1016/j.dt.2024.08.001
Vidakis N, Petousis M, Kalderis D, Michailidis N, Maravelakis E, Saltas V, Bolanakis N, Papadakis V, Argyros A, Mountakis N, Spiridaki M (2024d) A coherent engineering assessment of ABS/biochar biocomposites in MEX 3D additive manufacturing. Heliyon 10(11):e32094. https://doi.org/10.1016/j.heliyon.2024.e32094
Vidakis N, Petousis M, Kalderis D, Michailidis N, Maravelakis E, Saltas V, Bolanakis N, Papadakis V, Spiridaki M, Argyros A (2024e) Reinforced HDPE with optimized biochar content for material extrusion additive manufacturing: morphological, rheological, electrical, and thermomechanical insights. Biochar 6(1):37. https://doi.org/10.1007/s42773-024-00314-5
Wambua P, Ivens J, Verpoest I (2003) Natural fibres: can they replace glass in fibre reinforced plastics? Compos Sci Technol 63(9):1259–1264. https://doi.org/10.1016/S0266-3538(03)00096-4
Wang X, Zhao L, Fuh JYH, Lee HP (2019) Effect of porosity on mechanical properties of 3D printed polymers: experiments and micromechanical modeling based on X-ray computed tomography analysis. Polym (Basel). https://doi.org/10.3390/polym11071154
Wei X, Li D, Jiang W, Gu Z, Wang X, Zhang Z, Sun Z (2015) 3D Printable graphene composite. Sci Rep 5(1):11181. https://doi.org/10.1038/srep11181
Yan C, Kleiner C, Tabigue A, Shah V, Sacks G, Shah D, DeStefano V (2024) PETG: applications in modern medicine. Eng Regen 5(1):45–55. https://doi.org/10.1016/j.engreg.2023.11.001
Yasmin A, Daniel IM (2004) Mechanical and thermal properties of graphite platelet/epoxy composites. Polym (Guildf) 45(24):8211–8219. https://doi.org/10.1016/j.polymer.2004.09.054
Yuan L, Ding S, Wen C (2019) Additive manufacturing technology for porous metal implant applications and triple minimal surface structures: a review. Bioact Mater 4:56–70. https://doi.org/10.1016/j.bioactmat.2018.12.003
Zhang Q, Zhang D, Xu H, Lu W, Ren X, Cai H, Lei H, Huo E, Zhao Y, Qian M, Lin X, Villota EM, Mateo W (2020) Biochar filled high-density polyethylene composites with excellent properties: towards maximizing the utilization of agricultural wastes. Ind Crops Prod 146:112185. https://doi.org/10.1016/j.indcrop.2020.112185
Zhang Y, He M, Wang L, Yan J, Ma B, Zhu X, Ok YS, Mechtcherine V, Tsang DCW (2022) Biochar as construction materials for achieving carbon neutrality. Biochar 4(1):59. https://doi.org/10.1007/s42773-022-00182-x
Ziemian S, Okwara M, Ziemian CW (2015) Tensile and fatigue behavior of layered acrylonitrile butadiene styrene. Rapid Prototyp J 21(3):270–278. https://doi.org/10.1108/RPJ-09-2013-0086